Low-Power and Low-Noise Multi-Channel ASIC for X-ray and Gamma-Ray Spectroscopy

Sindre Mikkelsen [1], Dirk Meier [1], Gunnar Mæhlum [1], Bjørn Sundal [1], Jahanzad Talebi [1], Anders Helland [2], Nikolai Ostgaard [2], Yngve Skogseide [2], Kjetil Ullaland [2]

[1]*Gamma Medica-Ideas, Norway*
[2]*University of Bergen, Norway*

***Abstract*– The XA is an application specific integrated circuit (ASIC) for gamma- and X-ray energy spectroscopy. The circuit was designed to read signals from semiconductor radiation sensors such as cadmium zinc telluride (CZT) or cadmium telluride (CdTe). The assembly of CZT sensors with XA-ASICs allows one to measure energies of gamma- and X-rays in the range from 20 keV to 500 keV. The XA-ASIC contains 128 pre-amplifiers each followed by pulse shaping circuits and level comparators for triggering and address encoding. Upon interaction of radiation in the sensor the XA delivers an analog signal proportional to the energy of the gamma ray as well as a digital address corresponding to the pixel position. A total of 128 XA-ASICs (16384 channels) will be used in the Atmosphere Space Interaction Monitor (ASIM). ASIM will be mounted on the Columbus module of the International Space Station (ISS), from where it will study radiation phenomena over terrestrial thunderstorm regions. This article describes the XA-ASIC architecture and presents results from tests with CZT-based radiation detectors for ASIM.**

1 INTRODUCTION

1.1 Rationale for Mixed Mode ASICs in Gamma- and X-ray Radiation Detectors

Front-end electronics for nuclear radiation detectors and imaging systems is commonly implemented using discrete transistors and operational amplifiers where the size of electronic components ranges from a few millimeters to centimeters. The traditional gamma camera design, based on a NaI-scintillator and photomultiplier tubes, has about 50 electronic channels per quarter of a square meter (one tube corresponds to one electronic channel). Given the small number and low density of channels in traditional gamma cameras, the front-end readout implemented using discrete components is a natural solution. While traditional gamma cameras have only a small number of channels, today's X-ray imaging systems have ten thousand channels/cm^2 and visible light digital cameras have more than one million channels/cm^2. Due to the large number of channels in X-ray imaging systems and visible light digital cameras, front-end electronics is often implemented on the sensor or in its vicinity using integrated circuits with sub-micron feature size. Those imaging systems are read out by custom-made application specific integrated circuits (ASICs). These ASICs are designed and manufactured mainly in complementary metal-oxide-semiconductor (CMOS) technology. At large number and high density of channels the readout using discrete components becomes technically impossible and system costs are prohibitively high, while the readout with ASICs in CMOS technology meets the technical requirements at a much lower cost per channel. Unlike traditional gamma cameras, new imaging systems are being developed based on cadmium zinc telluride (CZT), mercuric iodine (HgI) or silicon photo sensors for scintillators. These new cameras have many electrodes, in the form of pixels or strips, often at sub-millimeter pitch and the front-end readout for these sensors is ideally implemented on ASICs. The readout of radiation sensors always combines analog and digital functions requiring a mixed mode design which allows the developers to integrate many functions on the same chip and thereby minimize overall system size and weight. ASICs allow the developer to optimize electronic performance because the parasitic capacitances on the ASIC can be lower than in discrete components which helps to improve the signal-to-noise ratio, increase the signal speed, and reduces the power dissipation.

1.2 Example of a Radiation Detector Test System with XA-ASIC Readout

The XA ASIC described here is a successor of ASICs previously developed for charged particle tracking with silicon sensors in high-energy physics experiments [1] and for the imaging of multiple radio-labeled isotopes on micro-arrays [2], [3], [4]. The XA front-end has been optimized for good performance with CdTe and CZT-based radiation sensors for single photon energy spectroscopy and imaging. The analog front-end is specified for CdTe and CZT sensors, but the concept of analog signal processing is valid for other semiconductor sensors, and allows the designer to adapt to other sensor parameters while retaining the same concept of analog signal processing. The XA-ASIC digital back-end is fairly general and meets the requirements of single photon emission computed tomography (SPECT) with small gamma cameras. Figure 1 (left) shows a photograph of a printed circuit board (PCB) with two XA-ASICs. The ASICs are wire-bonded to pads on the PCB. The PCB contains copper traces to connectors which lead to the radiation sensor

on one side and to the system electronics on the other side. The PCB has a size of 25 mm by 25 mm. The board can be easily connected to sensor module prepared with mating connectors. Using the same electronic readout, the system allows one to measure the performance of radiation sensors which is useful for the tests of new semiconductor materials [5]. Figure 1 (right) shows a CZT-based radiation sensor with XA readout underneath. There are four CZT crystals connected to one PCB with two XA-ASICs. Each CZT has 64 pixels at 2.46-mm pitch. The CZT is 5-mm thick and therefore absorbs about 80 percent gamma radiation at 140-keV. The setup was built to test the performance of various sensor materials and assembly configurations.

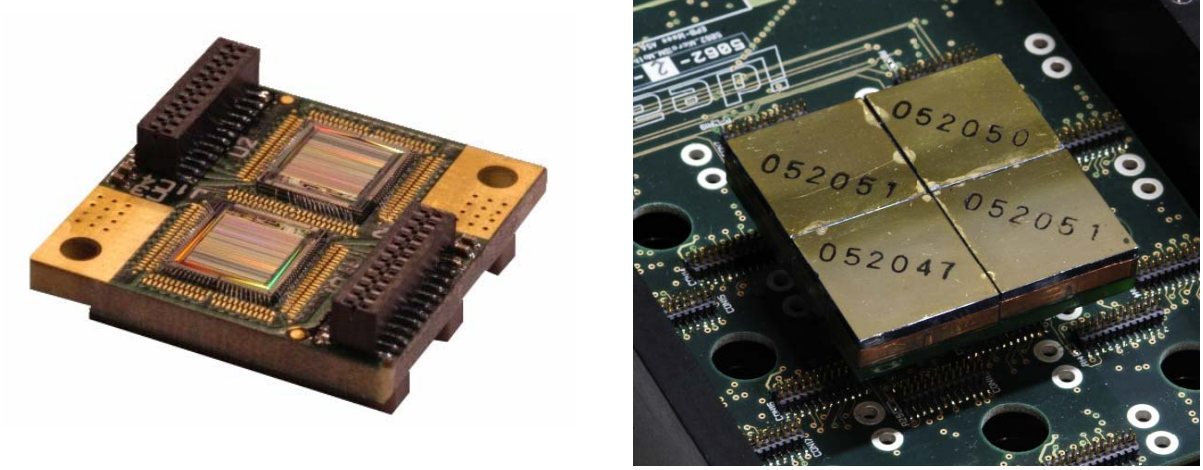

Figure 1: Left: photograph of a printed circuit board with two XA-ASICs. Right: photograph of a CZT-based radiation sensor array with XA readout underneath (not visible).

1.3 Example of XA-ASICs in Nuclear Medicine

Recently, Gamma Medica-Ideas introduced CZT-based gamma cameras made of radiation detector modules with integrated XA readout [6]. The modular design allows one to easily develop cameras of various size and shape, planar and non-planar. Various radiation collimators can be mounted in front of the camera depending on the imaging task. One configuration of radiation modules is applied for molecular breast imaging [7]. Other detector configurations are applied in pre-clinical small animal SPECT [8].

1.4 Example of XA-ASICs in Space

Predecessors of the XA-ASIC have been used for space applications in SWIFT [9], SuperAgile [10] and PLASTIC/STEREO [11] and are evaluated for future experiments: BepiColombo [12], [13], CREAM [14], and NEXT [15]. New applications in space might include the Atmosphere Space Interaction Monitor (ASIM). ASIM is an experiment proposed for the International Space Station (ISS) external facilities on the Columbus module. ASIM is aimed at the study of high-altitude optical emissions from the stratosphere and mesosphere, the Transient Luminous Events (TLEs: Red Sprites, Blue Jets, Elves) and the short lived (~1 ms) Terrestrial Gamma Flashes (TGFs). The TGFs are probably related to TLE and/or thunderstorms. The TGFs were discovered in 1994 by the BATSE instrument [16]. TGFs are X-ray bremssthrahlung produced by relativistic electrons, up to tens of Mega-electron-Volts [18], on their way out of the atmosphere. Modeling results combined with the BATSE measurements indicate a production altitude of 10 km to 40 km [17]. ASIM is the first mission designed to measure both lightning, TLEs and TGFs. The Modular X- and Gamma ray Sensor (MXGS) using CZT as detecting material is designed to make the most comprehensive measurements to date of the occurrence frequency and characteristics of TGFs. Together with optical instruments ASIM will resolve the connection between lightning, TLEs and TGFs. A total of 128 XA-ASICs (16384 channels) will be used for MSGX on ASIM. Important requirements on detector readout electronics for space applications include low power dissipation and radiation tolerance: the latest XA ASICs dissipate 0.5 mW/channel while they retain the same signal and noise performance like their predecessors. The radiation tolerance has been improved compared to previous designs by using 0.35 µm feature size.

2 SPECIFICATIONS OF THE XA-ASIC

2.1 Principle of Radiation Detection with CZT and XA-Readout

The XA-ASIC is ideally suited for the readout of electric charge from anodes of CdTe or CZT radiation sensors. Figure 2 shows a schematic drawing of a radiation detector module (left) and its electronic principle (right). The CZT is a relatively heavy semiconductor material (5.8-g/cm^3 mass density, and atomic numbers 48, 32, 52 for Cd, Zn, Te, respectively). Gamma- or X-rays illuminating the crystal are likely to interact and generate electron-hole pairs (4.6 eV per *eh*-pair in CZT). For example, a 122-keV gamma quant from Co-57 generates on average 26521 *eh*-pairs through photo absorption in CZT. The CZT crystal has a solid electrode (cathode) on one side and 256 pixels (anodes) on the other side. A detector bias voltage provides negative potential (-500 Volt) at the cathode and generates an electric field (1 kV/cm) inside the CZT crystal which causes the electrons to drift towards the anodes and thereby generate a small current. Each anode pixel is connected to a charge sensitive amplifier in the ASIC. Within 2 µs after the interaction in CZT, the ASIC delivers the charge amplitude at AMP, the address of the pixel at ADR and a trigger signal at TRG.

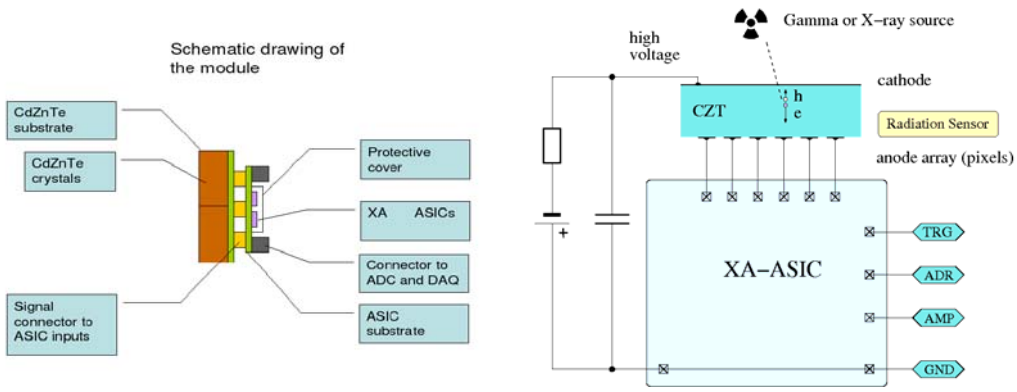

Figure 2: Schematic drawing of a radiation detector module with XA-ASIC readout (left) and the electronic principle of a pixelated CZT-based radiation sensor connected to XA-ASIC readout (right).

2.2 Basic Functionality of the XA-ASIC

Table 1 lists the basic functionality of the XA-ASIC and the concept of implementing it. The XA-ASIC has 128 inputs to channels of charge sensitive amplifiers. Each channel provides analog signal processing and delivers a signal whose amplitude is proportional to the charge measured at the amplifier input. The ASIC sparsifies the data which means that it only delivers signals with amplitudes that exceed the respective discriminating threshold. The discrimination of data by amplitude reduces the data rate to the acquisition system. There exist readout ASICs which provide all amplitude data or continuously sampled data which requires higher data transfer rates to the acquisition system and more computing power. The XA-ASIC provides the amplitude and the address of the triggering channel which corresponds to the energy and position of the interaction in the radiation sensor. The XA-ASIC is data-driven, which means that it delivers data without external trigger, hand-shake, or reset cycle.

Functionality	Concept of Implementation
Input: Readout of 128 radiation sensors/electrodes/strips/pixels	128 parallel and independent inputs channels, current input
Signal processing • 128 x amplitude spectroscopy • simultaneously and independent	128 channels of analog signal processing: • charge sensitive amplifiers CSAs, • Semi-Gaussian shapers, • peak-hold devices
Data sparsification	Amplitude discriminators and multiplexer
Output: Delivers • analog amplitude and • digital address	Delivery of data immediately after radiation event, without external hand-shake, “data driven” protocol

Table 1: Basic functionality of the XA-ASIC and the concept of implementation.

2.3 Electrical Performance Specifications

Table 2 lists the electrical performance specifications for the XA-ASIC. Each channel has an input linear dynamic range of up to -12.5 fC which allows it to measure energies up to 360 keV in CZT. At much higher energies the amplitude eventually saturates. Each channel dissipates 0.5 mW which amounts to 64 mW for the entire XA-ASIC. The input transistors dissipate most of the power in order to keep the noise low. The electronic noise of the pre-amplifier is 130 e + 20 e/pF. This noise is measured in equivalent noise charge at the nominal shaping time of 0.5-us. The noise increases linearly with the capacitive load at the input [19]. Other noise is caused by the detector leakage current and dielectrics of materials [20]. Apart from effects in the CZT, the noise limits the energy resolution from the sensor and determines the minimum triggering thresholds. Triggering thresholds typically can be set at 0.3 fC (10 keV in CZT) or higher. The maximum rate capability per XA-ASIC is 20 kHz (tested) and up to 100 kHz have been confirmed by simulation. The XA-ASIC analog front-end was designed for detectors with relatively small capacitance up to 10 pF per channel and relatively large negative leakage currents of up to -100 nA per channel.

Parameter	Value	Comment
Number of input channels	128	Readout for 128 pixels
Input charge linear dynamic range	0 .. -12.5 fC	Negative charge, readout of anodes
Power dissipation	0.5 mW/channel	64 mW total (nominal setting)
Electronic input noise of CSA	130 e + 20 e/pF	At 0.5 µs shaping time. Typical energy resolution is 5.5 keV FWHM at 122 keV in CZT pixels
Threshold, minimum	0.3 fC, negative charge	10 keV in CZT, individual adjustable for each channel
Rate capability, maximum	20 kHz .. 100 kHz per ASIC	Highest rate tested with this ASIC is 20 kHz, but 100 kHz was simulated successfully.
Detector capacitance	0 pF .. 10 pF	Optimized for 4pF
Detector leakage current	0 nA .. – 100 nA	Negative current into the amplifiers

Table 2: Electrical performance specifications of the XA-ASIC.

3 DESCRIPTION OF THE XA-ASIC

3.1 Layout, Dimensions and Padframe

Figure 3 (left) shows a photograph of the XA-ASIC on a printed circuit board (PCB) where the ASIC is wire-bonded to pads on the board. The inputs are arranged on three sides of the ASIC in the shape of a “horse-shoe”. This arrangement simplifies wire-bonding and routing on the PCB. Each pad has a size of 90 µm by 90 µm. The XA-ASIC is 0.7-mm thick and has an overall size of 7.4 mm by 8.0 mm. For the XA-ASIC design and its applications it is very important to minimize noise in the pre-amplifiers due to possible pick-up of charge from digital data lines. Pick-up has been minimized by separating the analog and digital sections and using different lines for analog and digital power. Following common practice, voltage power supplies have capacitive decoupling and the voltage drop along ground reference has been minimized. Figure 4 shows the pad frame of the XA-ASIC. Only pads necessary for normal operation are labeled.

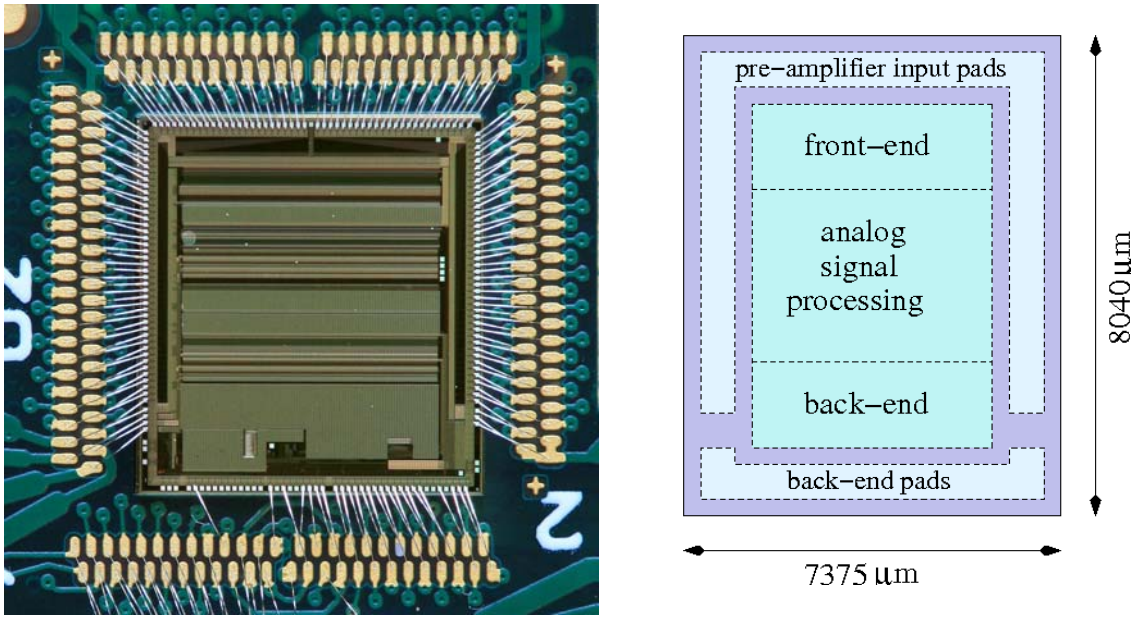

Figure 3: Photograph of the XA-ASIC mounted and wire-bonded to pads on a printed circuit board (left) and overview drawing of the XA-ASIC with dimensions (right).

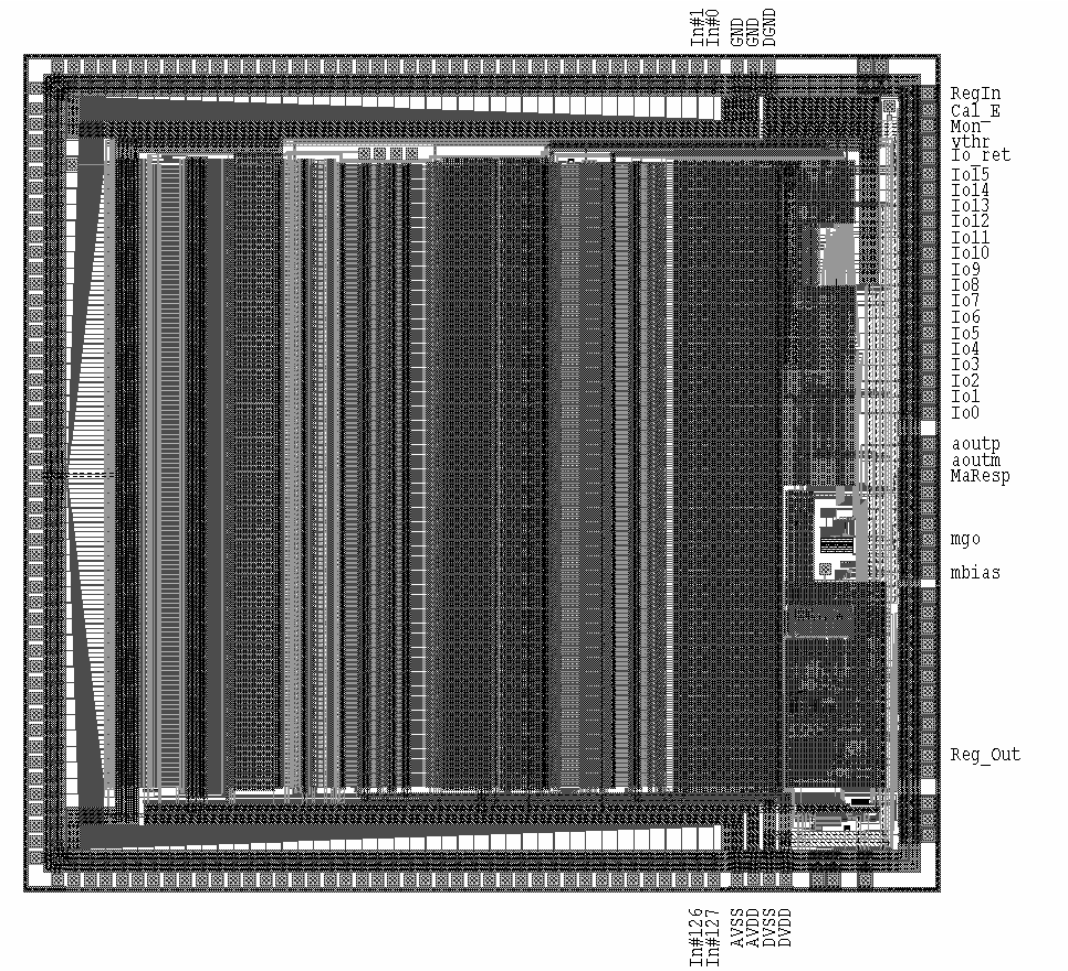

Figure 4: Padframe of the XA-ASIC.

3.2 Electrical Architecture

3.2.1 Overview and Backend

Figure 5 shows the electrical architecture of the XA-ASIC. The overview diagram contains four blocks: 1. the front-end, 2. the calibration network, 3. the bias generation network, and 4. the back-end. The front-end comprises 128 channels and one dummy channel (the channel is described in section 3.2.2 below). The dummy channel provides a reference voltage (*Vref*) to stabilize the output from other channels against variations of temperature and systemic noise (i.e. "common mode noise" caused by voltage variations in the power supply). Each of the 128 channels has a single-ended input (*In0..In127*) normally connected to an electrode of the radiation sensor or, in case of calibration, connected to the common node (*Cal*). The calibration network is a register which allows one to switch the input of any channel from their input pad to the *Cal* node. The state for each switch in the calibration network is stored in a register which is programmed by the user through data at *RegIn* and a clock at *Rck*. The bias generation network provides well defined bias currents and voltages to the circuitry in the front-end and in the back-end. The values are derived from one common node, *Mbias*, and from digital settings in the serial register. The current at *Mbias* must be applied by the user at an external pad. Each internal bias can be adjusted relative to its nominal value through digital-to-analog converters programmed by the user with data at *RegIn* and a clock at *Rck*. The back-end is connected to each channel via one line for amplitude and one line for triggers. Once a trigger occurs in any of the channels it passes on to the external *Trigger* node and internally multi-plexes the analog value to the output buffer. The output buffer subtracts the reference value, *Vref*, from the analog signal, and generates a differential current at *Outp* and *Outm*. The triggering channel number is encoded to the parallel *Address Out*. The back-end automatically generates a reset for the channels to be ready for the next radiation event ("hit" in the detector).

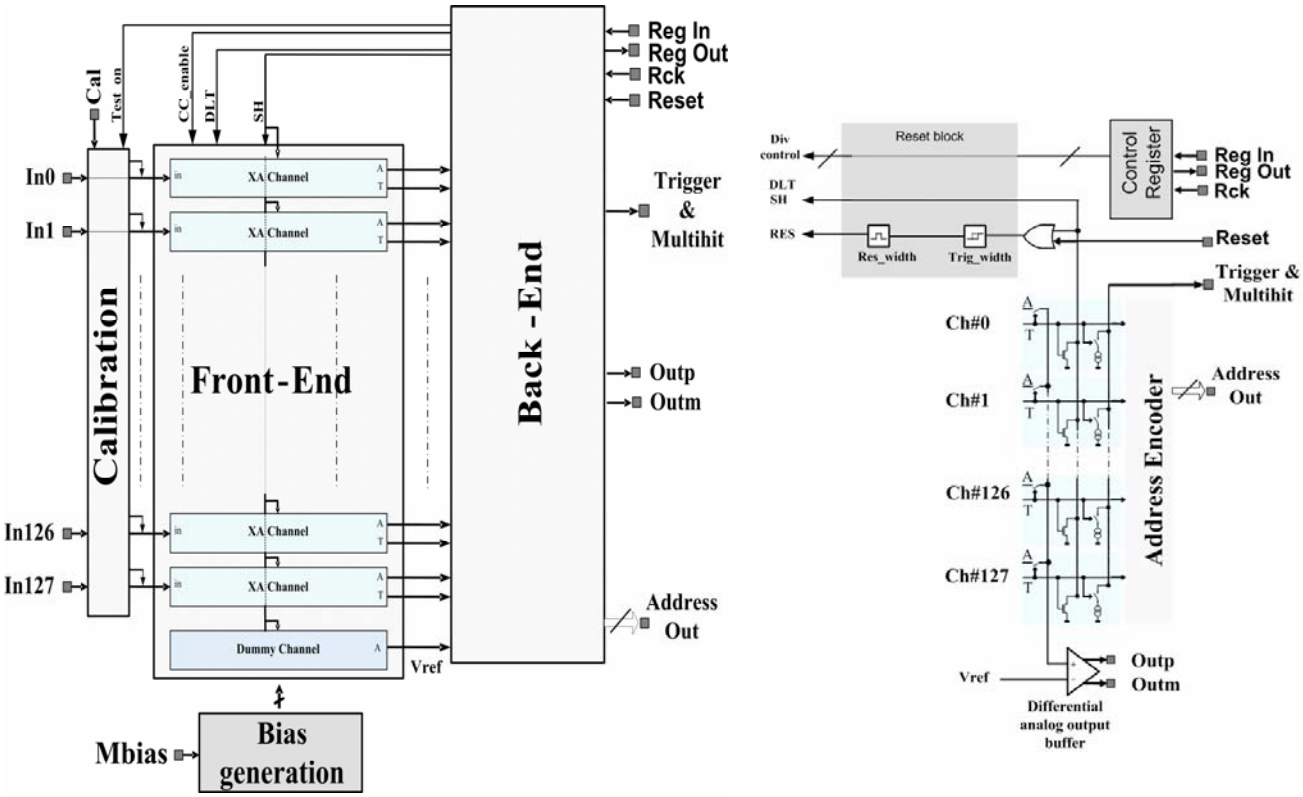

Figure 5: Electrical architecture of the XA-ASIC, with an overview (left) and the back-end (right).

3.2.2 Channel

Figure 6 shows the architecture of a channel in the XA-ASIC. The channel has one input, *In*, and two outputs *Analog Out*, and *Trigger*. A detector electrode, connected at *In*, delivers a current into the pre-amplifier. The current returns via ground to the detector bias voltage (not shown). The pre-amplifier has low input impedance and an input potential near ground. The pre-amplifier has a negative feed back via a capacitor, *Cfp*, and a resistor implemented by a field-effect transistor (FET). The feedback resistance can be controlled by the user through the bias *Vfp*. The pre-amplifier is followed by a shaper, a buffer and a peak hold device. The shaper is equivalent to a band pass filter to improve the signal-to-noise ratio. The shaper feeds an amplitude discriminator to generate triggers. The discriminator threshold can be programmed individually for each channel via digital-to-analog converters (DACs). The threshold DACs allow one to align all thresholds relative to each other and to compensate for different offset voltages which arise from process variations. The shaper and the peak hold device are automatically reset to their baseline after the analog values have been available for a nominal time of 2 μs. The XA has a master reset which can be applied externally by the user and resets all channels to zero amplitude.

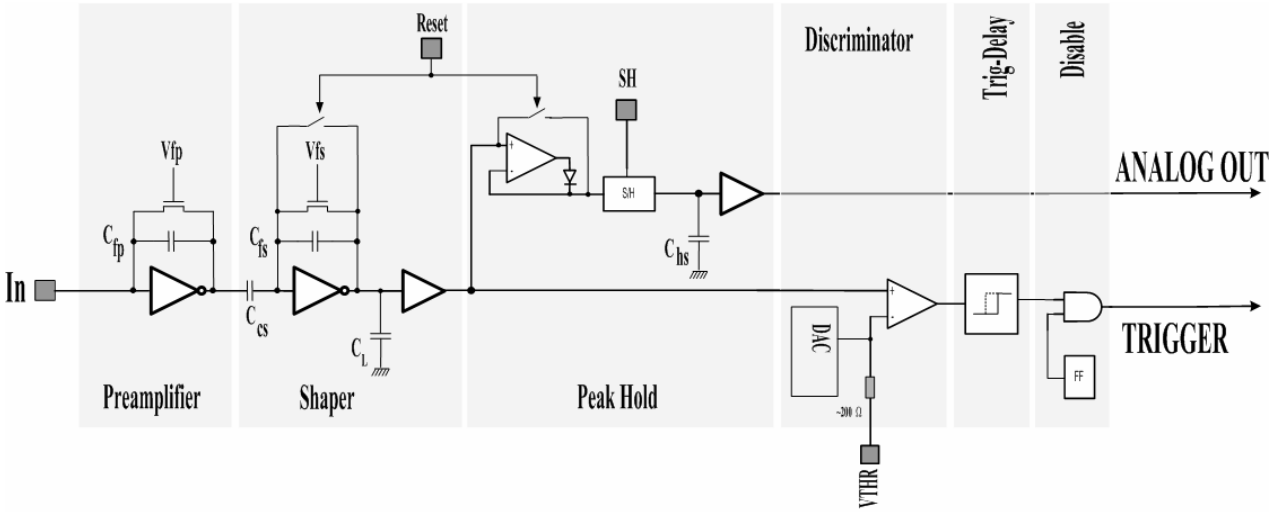

Figure 6: Architecture of a channel in the XA-ASIC.

3.2.3 Timing Diagram

Figure 7 shows a time diagram of important signals in a channel of the XA front-end. A short current pulse, *Iin*, flows from the sensor to the pre-amplifier input. Its duration is short compared to the nominal shaping time of 0.5 μs. The pre-amplifier output, *Preamp*, is a step with amplitude proportional to the time integral over the current *Iin*, equal to the charge delivered from the sensor. The step decreases slowly with a time constant determined by the feedback resistance and capacitance. The shaper forms a semi-Gaussian signal in order to improve the signal-to-noise ratio. The discriminator generates the *Trigger* as soon as the *Shaper* exceeds the *Threshold* (solid straight line). The amplitude is preserved at *Peak hold* (dashed straight line) and can be sampled internally for some time after the trigger. Due to the peak hold device, the timing of the *Trigger* and

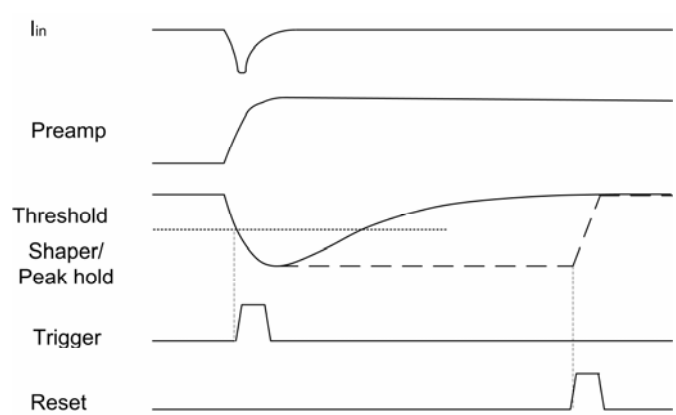

Figure 7: Timing diagram of signals in a channel.

sampling is non-critical – the sampled value is invariant under discriminator time walk or jitter.

Figure 8 shows the timing diagram of important signals in the back-end. The interaction of radiation in the detector, *Event*, causes the discriminator to trigger, *Int_trig*, which in turn activates sampling, *SH*. The sampled amplitude, *Aout*, becomes valid, as well as the binary address, *Adr_out*, and the *Trig_out*. The XA activates *RES* after some time in order to reset the shaper and the peak hold device. The duration between flanks of *Int_trig* and *SH* is nominally 1µs. The duration for active *SH* and valid *Aout*, *Adr_out*, and *Trig_out* is nominally 1µs. The XA-ASIC is "data driven" which means that it delivers data without external hand-shake. The data acquisition system must be designed to sample the data while it is valid.

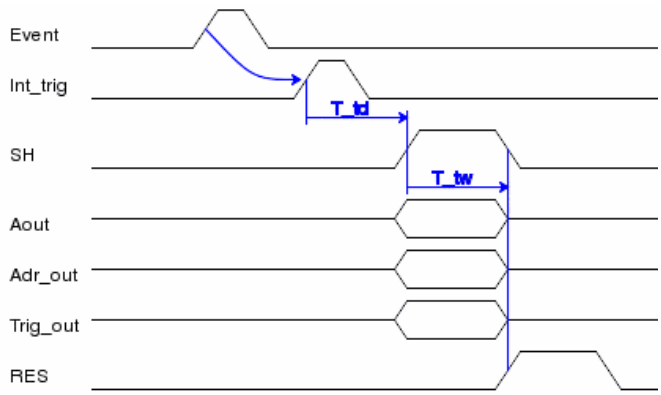

Figure 8: Timing diagram of signals in the back-end.

3.3 Important Features

The XA-ASIC provides several features which are important for many applications with radiation detectors. Table 3 gives an overview about these features and their implementation. The programmable register is a very convenient implementation which allows the user to control many internal parameters. The register is 858-bit long and can be programmed serially with data at *RegIn*, and a clock at *Rck*.

Features	Implementation
User can adjust internal bias values	programmable DACs
User can adjust all thresholds individually	programmable DACs
User can enable or disable channels	progammable configuration register
Amplitude calibration and test of functionality	internal capacitor, charge injection for all channels
Combine several ASICs	Common address bus and common analog line
Compensate change of external temperature	differential signals
Compensate large detector leakage current	current compensation network
Electrostatic Discharge (ESD) protection	diodes at the inputs , optimized for low-noise , resistors and diodes at the back-end
Radiation tolerance, prevent single event upset	Implemented in predecessors, see references [22], [21].

Table 3: XA ASIC features.

3.3.1 Bias Settings and Energy Thresholds

Bias currents and voltages are commonly used to define the operating point of FETs in ASICs. Each bias has a nominal value which is derived from a single main bias, *Mbias*. A nominal current of 500 µA should be applied at *Mbias*. In the XA, many biases can be applied by the user through external pads (see pad frame) or set through internal digital-to-analog converters (DACs). The DAC dynamic range and resolution has been designed to give the user flexibility to tune the parameters to the requirements. A programmed bias can be overwritten by directly driving the bias from the respective external pad. The external bias pads can be left unconnected under normal circumstances. The trigger threshold can be set by a DAC common for all channels. In addition thresholds can be tuned relative to the common threshold. Hence thresholds can be aligned by the user such that all channels trigger at the same energy.

3.3.2 Combine several ASICs

The XA design allows one to combine several ASICs. The ASIC's configuration registers are daisy chained via *RegIn* and *RegOut* to allow one to program all ASICs in the chain. The digital address bus and the analog amplitude output are connected in parallel. If the system has several ASICs on one data bus, then it is important to discard the data with an active *Multihit*. If several channels trigger within about 1 µs, the currents at *Multihit* sum up. The user can detect and count *Multihit* events and discard their address and analog value.

3.3.3 Stability versus Temperature and Supply Voltage

The XA has a few features which stabilize performance for varying temperature and supply voltage. Most variations cancel due to the differential output stage with the dummy channel. The stability of CZT with XA-ASICs has been studied in Reference [6].

3.3.4 Detector Leakage Current Compensation

The pre-amplifier inputs are connected to the electrodes of the radiation detectors either directly or via a capacitor. In case of direct coupling, the detector leakage current flows in the pre-amplifier input. The XA ASIC has a leakage current compensation circuit in order to keep the pre-amplifier operational at large leakage currents. Figure 9 shows a schematic drawing of the leakage current compensation circuit. The ASIC compensates for detector leakage current with an adaptive MOSFET current source at each preamplifier input. The MOS device is controlled by a slow differential amplifier, which senses the voltage difference between the input and the output nodes of the preamplifier. The leakage current compensation circuit is by default enabled, but it can be disabled by programming a bit in the configuration register.

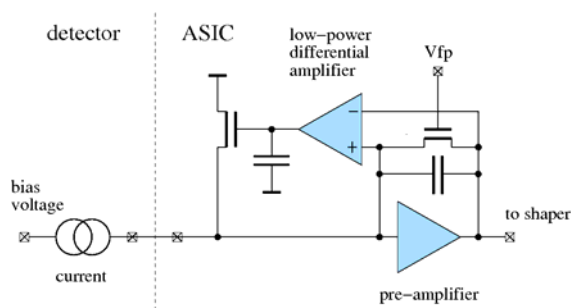

Figure 9: Schematic drawing of the current compensation circuit.

3.3.5 ESD Protection

Electrostatic discharge (ESD) may harm the ASIC in particular during manufacture, assembly and test. The XA-ASIC is protected against ESD by diodes at the pre-amplifier inputs and at all back-end outputs. Because standard ESD structures can add noise, the XA has customized diodes which retain the low noise performance and protect well against ESD. Some pads have additional series resistance build in to limit the current in case of ESD.

3.3.6 Amplitude calibration and test of functionality

The calibration network allows one to test the functionality of all channels and to measure their gain, the offset, the dynamic range and the discriminating threshold. The procedure assumes a sequence of well defined voltage steps applied to a capacitor to generate a charge at the *Cal* node. The user measures the mean output current at *Outp, Outm* for the known charge and thereby obtains the gain in units of output current over input charge. The user can sweep the voltage steps and hence measure the dynamic range.

3.3.7 Radiation Tolerance

The response of electronics under radiation is very important for applications in space and in many high energy physics experiments. Well known phenomena include radiation induced damage to the gate oxides of FETs as well as single event upset (SEU). ASICs have been irradiated with gamma radiation and a strong dependence on the design and manufacturing process has been observed. Radiation tolerance of similar circuits has been tested previously [21], and it was observed that radiation tolerance improves as the feature size decreases. The problem of SEU has been studied and solutions have been implemented in another ASIC [22]. These solutions have not yet been implemented in the XA-ASIC.

4 TESTS AND RESULTS

4.1 Experimental Setup

We prepared the test system hardware with one module according to Figure 1. The CZT crystal was manufactured for ASIM by reference [23]. We used a Co-57 radiation point source, fixed at about 1-m distance from the surface of the module. The gamma radiation illuminated the module uniformly. We acquired list mode data which contained the energy and the position of the radiation interacting in the module.

4.2 Energy Spectroscopy and Imaging

We analyzed the list-mode data using LabVIEW software. The analysis software computed the amplitude for each event in energy units of keV, and generated energy binned spectra for each pixel and images of counts in the pixels. Figure 10 (left) shows the energy spectrum measured from Co-57 in CZT summed for all 256 pixels. One can see the two characteristic photopeaks at 122 keV and 136 keV. Two important figures of merit are the energy resolution and the spectral shape. We measure an energy resolution of 5.4 keV full-width-at-half-maximum for 122 keV which is good. We observe a low-energy tail in the spectrum due to effects in the CZT sensor. Figure 10 (right) shows a count image in 256 pixels under uniform illumination. The image has regions with a high number counts (purple) and regions with lower counts (blue). The shape of the regions corresponds to the shape of the four crystals [Figure 1]. There are a few pixels on the edges of the crystals which do not trigger (black).

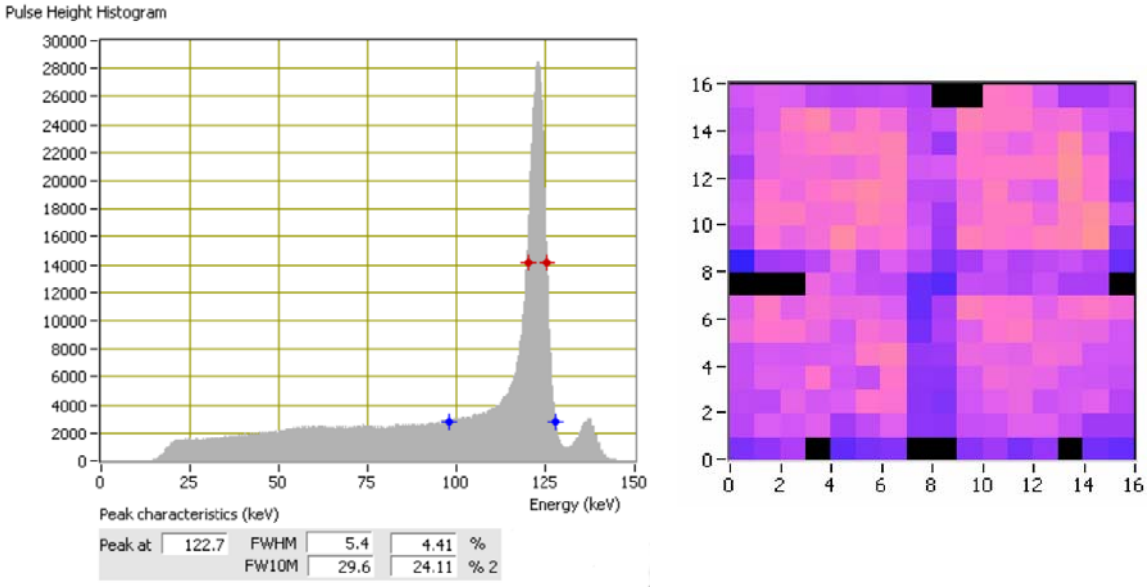

Figure 10: Energy distributions measured in 256 CZT-pixels under illumination with gamma rays from Co-57 (left) and count image in a CZT-based radiation detector, read out by two XA-ASICs (right).

5 ACKNOWLEDGEMENTS

We gratefully acknowledge funding from the Norwegian Space Centre (contract number VIT.01.06.1) and the ESA ELIPS 2, *European program for Life and Physical sciences and applications utilizing the International Space Station (ISS)*. Both, ESA and the Norwegian Space Centre, founded this development in order to supply the Atmosphere Space Interactions Monitor (ASIM) project with low noise, and low power front-end read-out electronics for the Modular X- and Gamma-ray Sensor (MXGS) experiment.

6 REFERENCES

[1] P. Aspell, R. Boulter, A. Czermak, P. Jalocha, P. Jarron, A. Kjensmo, W. Lange, E. Nygård, A. Rudge, O. Toker, M. Turala, H. Von Der Lippe, U. Walz, P. Weilhammer, and K. Yoshioka, "CMOS Low Noise Monolithic Front-Ends for Si Strip-Detector Readout", Nucl. Instr. Meth. A 315 (1992) 425-429.

[2] C. Ronnqvist, F. Santos, O. Toker, P. Weilhammer, K. Yoshioka, E. Nygard, A. Czermak, P. Jalocha, W. Dulinski, Y. Hu, "Double-Sided Silicon Microstrip Detectors and Low Noise Self-Triggering Multichannel Readout Chips for Imaging Applications", Nucl. Instr. Meth. A348 (1994) 440-443.

[3] A. Czermak, P. Jalocha, A. Kjensmo, C. Malamud, E. Nygard, C. Ronnqvist, F. Santos, J. Straver, P. Weilhammer, “A New 2-Dimensional High Resolution Si Detector for Beta- and Gamma-Radiography”, Nucl. Instr. Meth. A360 (1-2) (1995) 290-296.
[4] R. Turchetta, F.Anstotz, Y. Hu, J. P. Blonde, W. Dulinski, D. Husson and M. Schaeffer, “High Spatial Resolution Silicon Read-out System for Single Photon X-ray Detection”, IEEE Trans. Nucl. Sci. 41 (4) (6) (1994) 1063-1068.
[5] F. Quarati, R.A. Hijmering, G. Maehlum, A. Owens, E. Welter, “Evaluation of a CdZnTe Pixel Array for X- and G-ray Spectroscopy Imaging”, Nucl. Instr. Meth. A 568 (2006) 446-450.
[6] G. Maehlum, K.I. Dietzel, D. Meier, M. Szawlowski, B. Sundal, T. Vandehei, D.J. Wagenaar, “Study of Cadmium Zinc Telluride (CZT) Radiation Detector Modules under Moderate and Long-term Variations of Temperature and Humidity”, Proc. IEEE, Nucl. Sci. Symp. 2007, Vol. 2. 1645-1648.
[7] Michael O'Connor, Deborah Rhodes, Carrie Hruska, Stephen Phillips and Dana Whaley, “Molecular Breast Imaging (MBI) as an Adjunct to Screening Mammography”, J. Nucl. Med. 2008; 49 (Supplement 1):40P.
[8] S. Azman, J. Gjaerum, D. Meier, L.T. Muftuler, G. Maehlum, O. Nalcioglu, B.E. Patt, B. Sundal, M. Szawlowski, B.M.W. Tsui, D.J. Wagenaar, Y. Wang, “A Nuclear Radiation Detector System with Integrated Readout for SPECT/MR Small Animal Imaging”, Proc. IEEE, Nucl. Sci. Symp. 2007, 2311-2317.
[9] L.M. Barbier, F. Birsa, J. Odom, S.D. Barthelmy, N. Gehrels, J.F. Krizmanic, D. Palmer, A.M. Parsons C.M. Stahle, J. Tueller, “XA Readout Chip Characterization and CdZnTe Spectral Measurements”, IEEE, Trans. Nucl. Sci. 46(1), 7, 1999.
[10] Luigi Pacciani, Ennio Morelli, Alda Rubini, Marcello Mastropietro, Geiland Porrovecchio, Enrico Costa, Ettore Del Monte, Immacolata Donnarumma, Yuri Evangelista, Marco Feroci, Francesco Lazzarotto, Massimo Rapisarda, Paolo Soffitta, “SuperAGILE Onboard Electronics and Ground Test Instruments”, Nucl. Instr. Meth. A 574, (2007), 2, 330-341.
[11] A.B. Galvin et al., “The Plasma and Suprathermal Ion Compositioin (PLASTIC) Investigation on the STEREO Observatories”, Space Science Reviews, 136, 1-4, April 2008.
[12] Shin Watanabe, Shin’ichiro Takeda, Shin-nosuke Ishikawa, Hirokazu Odaka, Masayoshi Ushio, Takaaki Tanaka, Kazuhiro Nakazawa, Tadayuki Takahashi, Hiroyasu Tajima, Yasushi Fukazawa, Yoshikatsu Kuroda, Mitsunobu Onishi, “Development of Semiconductor Imaging Detectors for Si/CdTe Compton Camera”, Nucl. Instr. Meth., A 579 (2007) 871–877.
[13] Shin’ichiro Takeda, Shin Watanabe, Takaaki Tanaka, Kazuhiro Nakazawa, Tadayuki Takahashi, Yasushi Fukazawa, Hajimu Yasuda, Hiroyasu Tajima, Yoshikatsu Kuroda, Mitsunobu Onishi, Kei Genba, “Development of Double-Sided Silicon Strip Detectors (DSSD) for a Compton Telescope”, Nucl. Instr. Meth. A 579 (2007) 859–865.
[14] M.G. Bagliesi, C. Avanzini, G. Bigongiari, A. Caldarone, R. Cecchi, M.Y. Kim, P. Maestro, P.S. Marrocchesi, F.Morsani, R. Zei, “Front-end electronics with large dynamic range for space-borne cosmic ray experiments”, Nucl. Phys. Proc. Suppl. 172:156-158, 2007.
[15] H. Tajima, T. Kamae, G. Madejski, T. Mitani, K. Nakazawa, T. Tanaka, T. Takahashi, S. Watanabe, Y. Fukazawa, T. Ikagawa, J. Kataoka, M. Kokubun, K. Makishima, Y. Terada, M. Nomachi, and M. Tashiro, “Design and Performance of the Soft Gamma-Ray Detector for the NeXT Mission”, IEEE Trans. Nucl. Sci. 52, 6, (2005), 2749.
[16] G.J. Fishman, P. N. Baht, R. Mallozzi, J. M. Horack, T. Koshut, C. Kouveliotou, G. N. Pendleton, C. A. Meegan, R. B. Wilson, W. S. Paciesas, S. J. Goodman, and H. J. Christian, “Discovery of Intense Gamma-Ray Flashes of Atmospheric Origin”, Science, 164, 1313, 1994.
[17] N. Ostgaard, T. Gjesteland, J. Stadsnes, P. H. Connell, and B. Carlson, “Production Altitude and Time Delays of the Terrestrial Gamma Flashes: Revisiting the Burst and Transient Source Experiment Spectra”, J. Geophys. Res., 113, A02307, 2008.
[18] D.M. Smith, L.I.Lopez, R.Lin and C. P. Barrington-Leigh, Science, Vol 307, 2005.
[19] E. Nygard, P. Aspell, P. Jarron, P. Weilhammer and K. Yoshioka, “CMOS Low Noise Amplifier for Microstrip Readout Design and Results”, Nucl. Instr. Meth. A301 (1991) 506-516.
[20] D. M. Pettersen, S. Mikkelsen, J. Talebi, and D. Meier, “A Readout ASIC for SPECT”, IEEE Trans. Nucl. Sci. 52, 3, 2005.
[21] H. Aihara, M. Hazumi, H. Ishino, J. Kaneko, Y. Li, D. Marlow, S. Mikkelsen, D. Nguyen, E. Nygaard, H. Tajima, J. Talebi, G. Varner, H. Yamamoto, M. Yokoyama, “Development of Front-end Electronics for Belle SVD Upgrades”, Proc. IEEE, Nucl. Sci. Symp. 2, 9, 213, 2000.
[22] Samo Korpar, Peter Krizan, Sasa Fratina, “SEU Studies of the Upgraded Belle Vertex Detector Front-End Electronics”, Nucl. Instr. Meth., A 511 (2003) 195–199.
[23] Redlen Technologies, http://www.redlen.com/, Canada.